Conference on Modelling Fluid Flow (CMFF'06)
The 13th International Conference on Fluid Flow Technologies
Budapest, Hungary, September 6-9, 2006

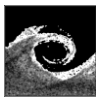

COMBINED EFFECTS OF CONTROLLED VORTEX DESIGN AND FORWARD BLADE SKEW ON THE THREE-DIMENSIONAL FLOW IN AXIAL FLOW ROTORS

János VAD[1], Ali R. A. KWEDIKHA[2], Csaba HORVÁTH[3]

[1] Corresponding Author. Department of Fluid Mechanics, Budapest University of Technology and Economics. Bertalan Lajos u. 4 – 6, H-1111 Budapest, Hungary. Tel.: +36 1 463 2464, Fax: +36 1 463 3464, E-mail: vad@ara.bme.hu
[2] Department of Fluid Mechanics, Budapest University of Technology and Economics. E-mail: kwedikha@ara.bme.hu
[3] Department of Fluid Mechanics, Budapest University of Technology and Economics. E-mail: csaba_h@hotmail.com

ABSTRACT

Comparative studies have been carried out on two axial flow fan rotors at their design flow rate in order to investigate the combined effects of controlled vortex design and circumferential forward skew on blade aerodynamics. The studies were based on Computational Fluid Dynamics, with composition and application of structured hexahedral grids taking up the challenge of the relatively complicated blade geometries due to skew and sweep. The computations indicated that the forward-skewed blade tip modifies the inlet flow field, leading to the rearrangement of spanwise blade load distribution, increase of losses along the dominant part of span, and converting the original non-free vortex spanwise blade circulation distribution toward a free-vortex flow pattern. The radial outward flow on the suction side, being especially significant for non-free vortex rotors, was found to be effectively moderated by forward skew, together with the losses associated. It has been concluded that forward skew is especially recommended for non-free vortex rotors for retardation of tip stalling.

Keywords: axial flow turbomachinery, blade skew, CFD, controlled vortex design

NOMENCLATURE

$C_p = (p-p_\infty)/(\rho u_t^2/2)$ [-] static pressure coefficient
S [-] fraction of span (S = 1: casing)
p [Pa] static pressure
Δp_t [Pa] total pressure rise
u [m/s] circumferential speed
v [m/s] absolute velocity
Φ [-] flow coefficient (annulus area-averaged axial velocity divided by u_t)
Ψ [-] total pressure coefficient (annulus mass-averaged total pressure rise divided by $\rho u_t^2/2$)
$\varphi = v_x / u_t$ [-] local axial flow coefficient
$\varphi_r = v_r / u_t$ [-] local radial flow coefficient
$\psi = \Delta p_t/(\rho u_t^2/2)$ [-] local total pressure coefficient
ρ [kg/m^3] fluid density
$\omega = \psi_{id} - \psi$ [-] total pressure loss coefficient

Subscripts and Superscripts
1 rotor inlet
2 rotor outlet
id ideal (inviscid)
r, x, u radial, axial, tangential
t blade tip
^ pitchwise-averaged
∞ far upstream

1. INTRODUCTION

Rotors of axial flow turbomachines are often of "controlled vortex" design (CVD) [1]. This means that contrarily to the classic free vortex concept prescribing spanwise constant design blade circulation, the circulation – and thus, the Euler work – increases along the dominant part of the blade span in a prescribed manner. CVD guarantees a better utilisation of blade sections at higher radii. By their increased contribution to the rotor performance, rotors of high specific performance can be realised, i.e. relatively high flow rate and total pressure rise can be obtained even with moderate diameter, blade count, and rotor speed [2]. CVD also gives a means for reduction of hub losses by unloading the blade root [3], and offers a potential to avoid highly twisted blades [4]. Furthermore, in multistage machinery, it is a means to realise an appropriate rotor exit flow angle distribution [1].

Blade sweep, dihedral, and skew are known as techniques of non-radial blade stacking. A blade has sweep and/or dihedral if blade sections of a datum blade of radial stacking line are displaced parallel

and/or normal to the chord, respectively [5]. A blade is swept-forward if the sections of a radially stacked datum blade are shifted parallel to their chord in such a way that a blade section under consideration is upstream of the neighbouring blade section at lower radius [2].

A special combination of dihedral and forward sweep is referred to as circumferential forward skew (FSK) [6]. In this case, the datum blade sections are shifted in the circumferential direction, toward the direction of rotation. By this means, the axial extension of the datum blading can be retained, the blade mechanics is expected to be more favourable than in case of forward sweep alone, and the following benefits, dedicated to the incorporated forward sweep, can be utilised. Forward sweep/skew offers a potential for improvement of efficiency [7], increase of pressure peak and extension of stall-free operating range [2][7], and noise reduction [6].

The literature reports extensively on FSK rotors of CVD, e.g. [3][6][7]. In these cases, the CVD design style is documented without further discussion, and the study concentrates on the skew-related effects. However, no special emphasis is given to the combination and interaction of three-dimensional (3D) flow phenomena due to CVD and FSK. This paper aims to contribute to a more comprehensive understanding of such combined effects, in order to aid the designer with guidelines for incorporation of FSK in the CVD technique. To this end, two comparative rotors of CVD, an unskewed (USK) and a FSK one, are studied in the paper at the design flow rate, by means of Computational Fluid Dynamics (CFD).

2. ROTORS OF CASE STUDY

A preliminary study of this work is documented in [8], in which the rotors have been presented in detail. Therefore, only a short account is given here.

The FSK rotor, together with outlet guide vanes, was designed by Vad [8]. It operates in the low-speed wind tunnel facility of the Hungarian Institute of Agricultural Engineering, Gödöllő, Hungary. The main geometrical data and design operational characteristics of the FSK rotor are presented in Table 1.

FSK was originated from the virtual USK rotor of radial stacking line. The blade sections of USK are shifted in circumferential direction toward the direction of rotation in order to obtain FSK, without making any modifications to the blade section geometry. The circular-arc cambered blade sections have C4 (10 %) profiles along the entire span. The trailing edges (TEs) of both USK and FSK fit to planes normal to the axis of rotation.

A virtual image of FSK, obtained from the CFD technique, is shown in Figure 1. The skew angle is defined as the angle between radial lines fitted to the TEs of the datum and to the shifted blade sections at a given radius, and is positive if the skew is applied in the direction of rotation (forward skew). As the figure illustrates, the skew angle is zero at the hub and increases progressively along the span, similarly to the style applied in [7]. By this means, it was intended to avoid any stacking line blend points, for which increased losses may be expected [9]. Geometrical details of the blading are specified in Table 2. The blades have backward sweep of leading edge (LE) near the hub, resulting in positive sweep [5] as a potential means of hub loss reduction.

Table 1. FSK rotor main characteristics

Casing diameter	2000 *mm*	Φ	0.33
Hub-to-tip ratio	0.6	Ψ	0.27
Blade count	12		
Tip clearance (% span)	5 %		

Figure 1. Isometric view of FSK

Table 2. Geometrical details of FSK blading

S	**0 hub**	**0.25**	**0.50 mid**	**0.75**	**1.00 tip**
Solidity	1.38	1.01	0.89	0.80	0.72
Camber angle, deg	20.3	17.3	16.8	15.8	15.3
Stagger angle, deg*	33.9	32.1	30.7	29.9	29.4
Skew angle, deg	0.0	0.0	0.3	1.6	3.5

*Measured from circumferential direction

3. CFD TECHNIQUE

The flow fields in USK and FSK were simulated by means of the commercially available finite-volume CFD code FLUENT [10]. Referring to e.g. [11] reporting on computations regarding swept and leaned compressor rotors, the standard *k-*ε turbulence model [12] has been used, with enhanced wall treatment of FLUENT. The main feature of this wall treatment is that it is a blended

model between the two-layer model and the logarithmic law of the wall [13].

With consideration of periodicity, the computations regarded one blade pitch only. A typical computational domain is presented in Figure 2. The domains extend to approx. 8 and 3,5 midspan axial chord lengths upstream and downstream of the rotor blading in the axial direction, respectively. The inlet face is a sector of the circular duct with a 30 deg central angle. Downstream of the inlet face, sectors of the steady inlet cone and the rotating hub with one blade in the middle of the domain are included for both types of blading.

At the inlet face, swirl-free uniform axial inlet condition corresponding to the design flow rate has been prescribed. The inlet turbulence intensity has been set to 1 percent, and the casing diameter was taken as the hydraulic diameter for the calculation of the turbulence length scale. Utilising the features of the annular cascade configuration, boundary conditions of periodicity were applied. A zero diffusion flux condition has been used for all flow variables at the outlet boundary (outflow condition in FLUENT [10]).

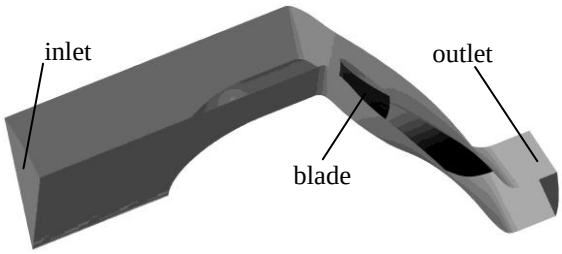

Figure 2. Typical computational domain

Taking e.g. [11] and [14] as preliminary references, a structured fully hexahedral mesh has been developed for the entire computational domain. Following the guidelines in [15] emphasizing the necessity of good grid quality, this meshing technique is felt promising from the viewpoint of computational accuracy. Furthermore, it offers a means to reduce the computational cost by moderating the cell size – although the investment in manpower is significant during mesh composition.

The mesh of the outer domain consists of 202, 26, and 48 grid points in axial, circumferential, and spanwise directions, respectively. The total number of the applied hexahedral cells is approximately 470.000, with about 50 % of cells in the refined domain in the vicinity of the blade. The tip clearance is resolved using 8 grid points, with meshing technique similar to the one applied in [16]. Taking up the challenge of relatively complicated blade geometry due to skew above midspan and LE sweep near the hub, the domain consists of 31 blocks. Figure 3 presents the mesh for FSK near the LE and the TE. An enlarged view of the mesh near the LE at the hub, composed to meet the challenge of LE sweep, is also shown in the figure, from another perspective in order to get better visibility.

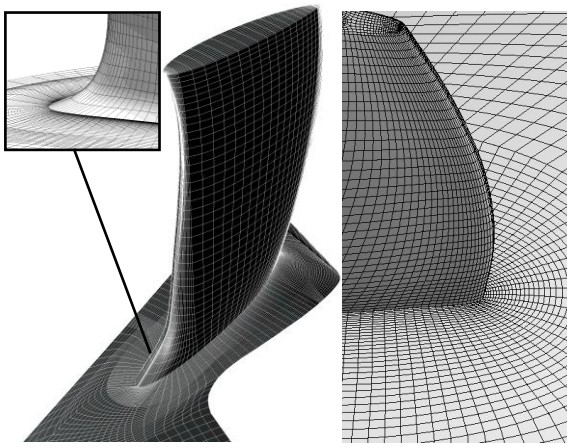

Figure 3. Mesh for FSK near the LE and TE

A C-type mesh topology has been built around the LE and TE, while H-type topology is applied to the entire rotor blade passage. Figure 4 presents an example of the C-type meshing topology, ensuring smooth meshing gradient in the pitchwise direction from blade suction surface towards the periodic boundary.

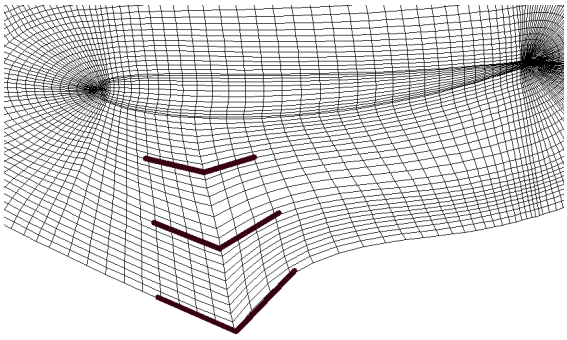

Figure 4. Example for meshing details

The equiangle skewness of a cell is defined as the maximum value of the ratio of actual and possibly highest deviation from the optimum angle, considering each vertex [10]. The grid ensures that 99 % of the cells have equiangle skewness less than 0.7, and the maximum skewness value is 0.82.

During the computations, the majority of y^+ values fell within the range of 15 to 100, fulfilling the requirements of the applied wall law.

The discretisation of the convective momentum and turbulent quantity fluxes were carried out by the Second Order Upwind method. Typical computations required approximately 3000 iterations. The solutions were considered converged

when the residuals of all equations were resolved to levels of order of magnitude of 10^{-6}.

The computations presented here are valid for a rotor speed of 416 RPM. The Reynolds number, calculated with the blade tip speed, the tip chord and the kinematic viscosity of air at 20 °*C* is $1.074 \cdot 10^6$. The Mach number computed with the blade tip velocity and the speed of sound in air at 20 °*C* is 0.13 and therefore, the flow is considered incompressible.

Measurements carried out on FSK available in the Gödöllő wind tunnel facility will serve in the future as a basis for experimental validation of the CFD technique [8]. These experiments regard characteristic curve measurements as well as hot wire anemometer studies upstream and downstream of FSK. The experimental technique and the results will be reported in a later paper. At the time of submission of this paper, no processed and evaluated hot wire measurement data are available.

Characteristic curve measurements were carried out and reported in [8]. At the design point of Φ = 0.33, the measurements resulted in a total pressure rise of Ψ = 0.27. The presented computational technique resulted in Ψ = 0.26. The preliminary processing of hot wire measurement data on the outlet axial velocity profile showed that the computational technique resolves the hub boundary layer well. The spanwise gradient of outlet axial velocity due to non-free vortex operation and the location of peak axial velocity is also well captured.

4. DISCUSSION OF RESULTS

4.1. Pitchwise-Averaged Data

Figure 5 presents the spanwise distribution of pitchwise averaged values for the dimensionless inlet and outlet axial velocities, outlet radial velocity, outlet ideal total pressure rise, and the total pressure loss coefficient at the outlet. The inlet and outlet planes have the axial position of -0.2 and 1.13 % midspan axial chord, respectively, where the zero axial position indicates the LE at midspan. The ideal total pressure rise has been calculated from the Euler equation of turbomachines, considering swirl-free inlet: $\Delta p_{t\,id} = \rho\, u\, c_{u2}$.

The diagrams suggest the following. The applied blade skew has an influence already on the inlet flow field: the inlet axial velocity for FSK is increased near the tip and is reduced at lower radii. The outlet axial velocity is increased at lower radii for FSK. The difference in radial rearrangement of fluid for USK and FSK is visible on the outlet radial velocity plot. As the ideal total pressure plots suggest, FSK performs also increased Euler work along the dominant part of span. The diagrams show that both the ideal total pressure rise and the outlet axial velocity increase along the dominant part of span, as a consequence of the CVD concept [17]. Although the total pressure loss is reduced near the tip, it is increased over the dominant part of span due to skew. The same tendency was reported in [9] for a rotor with forward sweep at the tip.

The above tendencies will be explained in the following section, by means of analysis of the detailed flow field. Inlet and outlet flow maps will be presented. Furthermore, the flow field will be surveyed at 30 and 90 % span, being two representative locations where significant differences occur in the fluid mechanical behaviour of USK and FSK (see Fig. 5).

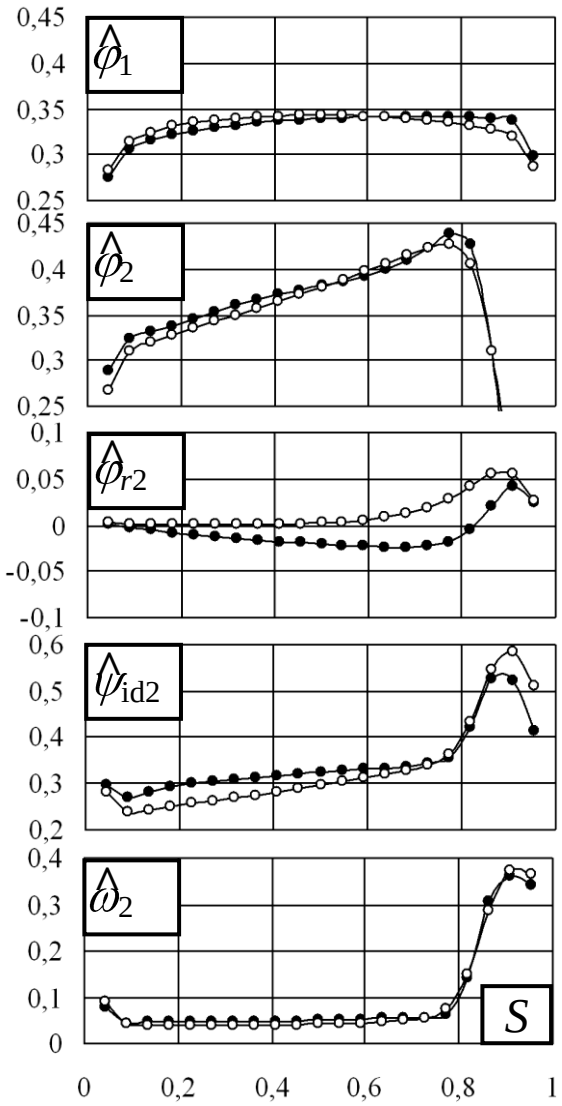

Figure 5. Pitchwise-averaged data. White dots: USK, black dots: FSK

4.2. Flow Details

For the bladings discussed herein, the chordline makes a relatively small angle with the circumferential direction (see Table 2). This suggests that the effect of forward sweep dominates over that of dihedral in the aerodynamics of FSK.

Figure 6 shows the inlet axial velocity maps. A zone of increased inlet axial velocity is observed

near the tip of FSK. The reason is that the near-tip part of the forward skewed blading protrudes into the upstream relative flow field, and carries out work "in advance" compared to the blade sections at lower radii. According to the conservation of mass at the prescribed design flow rate, this results in the reduction of inlet axial velocity at lower radii of FSK, as was already indicated in Fig. 5.

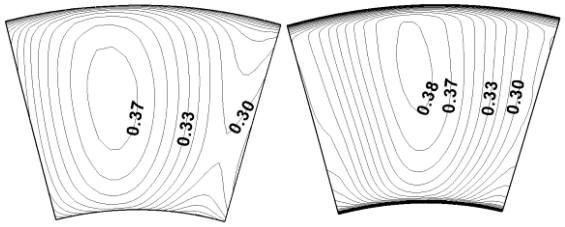

USK, φ_1 **FSK, φ_1**

Figure 6. Inlet axial velocity field

The reduced axial velocity at lower radii of FSK results in increased incidence, manifesting itself in increased lift, i.e. increased depression and overpressure on the suction side (SS) and pressure side (PS), respectively. This is illustrated in the static pressure plots of Figure 7.

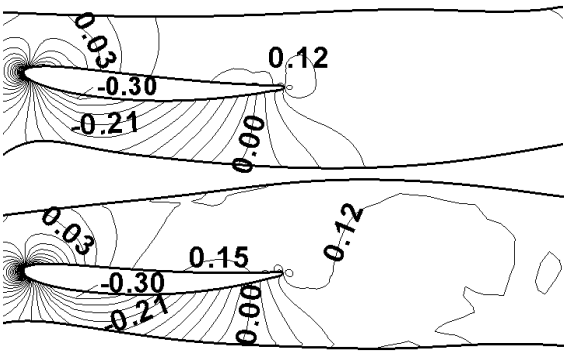

Figure 7. Static pressure coefficient C_p at 30 percent span. Upper: USK, lower: FSK

As [9] also suggests, the higher lift being valid for FSK at lower radii potentially leads to increased Euler work and blade section performance. Indeed, as Figures 8 and 9 indicate, FSK performs higher ideal total pressure rise and axial velocity in the aft-LE region, compared to USK, as was suggested already by Fig. 5.

The increase of axial velocity for FSK in the aft-LE region can be explained by taking a look on the isobar lines on the SS in Figure 10. Due to forward skew, the isobars in the decelerating region are inclined "more forward" for FSK than for USK. Therefore, the local radial outward flow is moderated, the flow is guided "more inward" for FSK on the SS, as also illustrated in Figure 11. The radial flow controlling effect of forward skew has been described qualitatively in [7], with special regard to the flow in the SS boundary layer, but regardless the control of flow in the entire blade passage. According to the conservation of mass, the moderation of radial outflow leads to the increase of the axial velocity at lower radii. The "inward-guiding" effect on the flow due to forward skew, which already appeared in the outlet radial velocity plot of Fig. 5, is observable also on the PS, as Figs. 9 and 11 suggest.

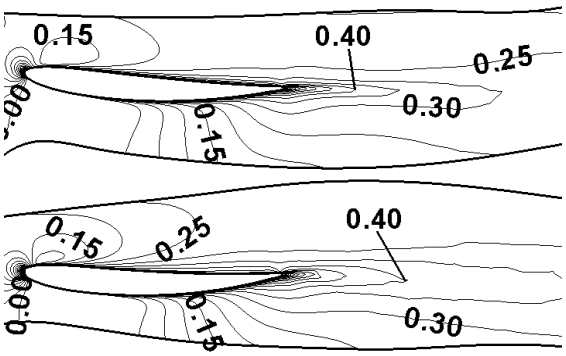

Figure 8. Ideal total pressure rise coefficient ψ_{id} at 30 percent span. Upper: USK, lower: FSK

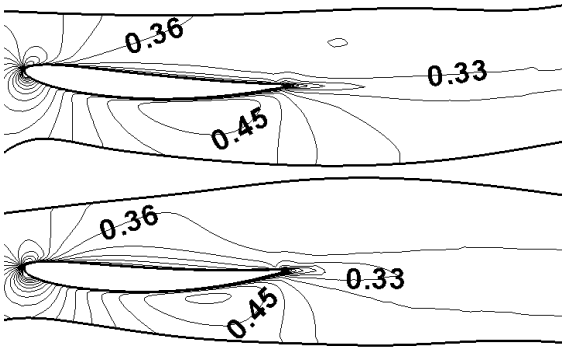

Figure 9. Axial flow coefficient φ at 30 percent span. Upper: USK, lower: FSK

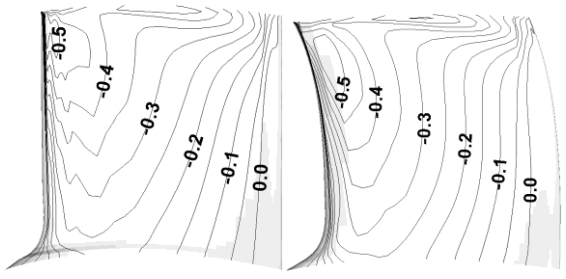

Figure 10. Distribution of static pressure coefficient C_p on the SS. Left: USK, right: FSK

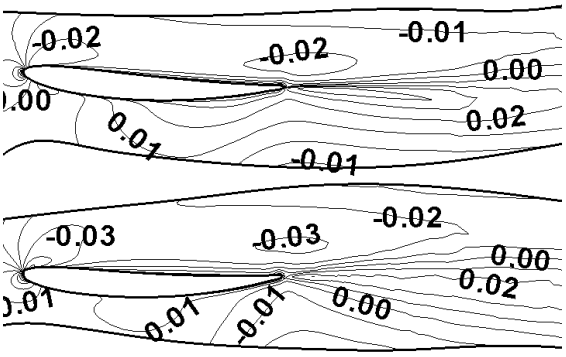

Figure 11. Radial flow coefficient φ_r at 30 percent span. Upper: USK, lower: FSK

As Figure 12 shows, the increased incidence at lower radii of FSK results in higher losses. Such increase of loss due to skew occurs along the dominant part of span, as presented in Fig. 5.

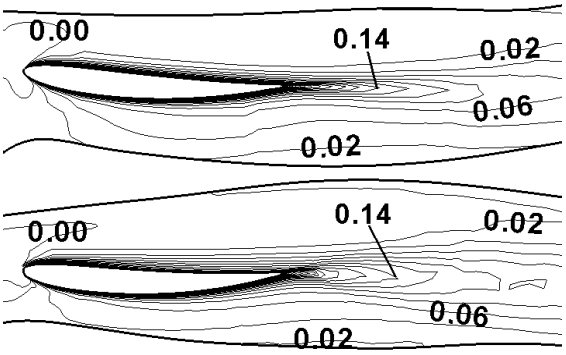

Figure 12. Total pressure loss coefficient ω at 30 percent span. Upper: USK, lower: FSK

In the following, the flow phenomena near the tip are analysed. The loss-reducing effect of forward skew in the near-tip region is apparent in Figure 13, where a "loss trough" of reduced losses and extension can be observed for FSK. Besides this, it must also be noted that not only the losses but also the Euler work has been reduced due to skew near the tip (Fig. 5). Figure 14 shows appropriately selected isosurfaces of radial flow coefficient and total pressure loss coefficient in the near-tip region. It is apparent in the figure that the reduction of radial outward flow due to forward skew leads also to the reduction of loss. Both tendencies can be seen in Fig. 5.

The following comments regard the 3D flow features due to CVD. Fig. 15 presents the maps of flow characteristics at the outlet section. The blade wake is located in the middle, with the PS and SS on the left and right, respectively. The figure demonstrates that the ideal total pressure rise increases along the dominant part of span of USK, in accordance with the CVD concept. However, an inevitable and undesired consequence of CVD is that vortices are shed from the TE, generating a characteristic 3D flow pattern in the blade passage [17]: radial inward and outward flow on the PS and on the SS, respectively. By means of forward skew, the shed vorticity has been moderated along the dominant portion of span. However, as Fig. 5 illustrates, the moderation of shed vorticity acts against the non-free vortex design concept: the spanwise gradient of blade circulation – and that of the related ideal total pressure rise – tends to be reduced toward free vortex operation.

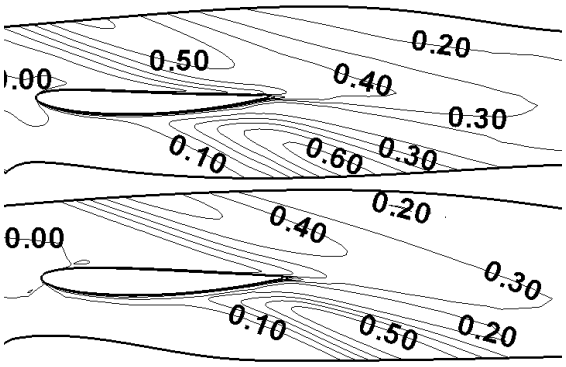

Figure 13. Total pressure loss coefficient ω at 90 percent span. Upper: USK, lower: FSK

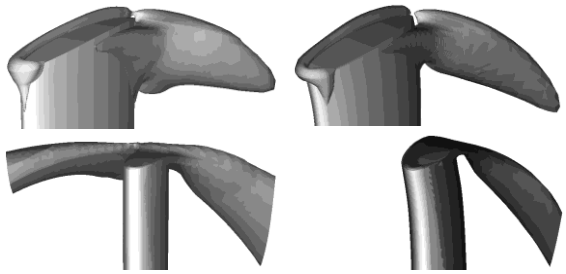

Figure 14. Upper row: φ_r = 0.1 isosurfaces. Lower row: ω = 0.5 isosurfaces. Left: USK, right: FSK

5. REMARKS

5.1. Forward Sweep/Skew vs. Losses

The technical literature reports apparently contradictory results on the loss and performance modifying effects due to forward sweep/skew. In [5], it is pointed out that forward sweep near the tip, i.e. "positive sweep", gives a potential for reduction of near-tip losses. Based on [7], application of near-tip forward skew can be recommended for efficiency improvement over the entire operational range, and for stall margin improvement. [2] and [6] suggest that the application of forward sweep along the entire span is beneficial for loss reduction and performance improvement, and also for extension of stall-free range. However, it has been found in [9] that forward sweep causes the deterioration of efficiency near the design point, although it was

found beneficial at throttled (near-stall) operating points. In [18], the reduction of efficiency was reported for a forward-swept rotor over the dominant part of the entire stall-free operational range.

This paper gives an additional example, together with a detailed explanation, how forward skew may cause the increase of losses at the design flow rate over the dominant portion of span, although it must be acknowledged that the losses are reduced near the tip. It must also be emphasized that in energetic judgment of a skewed rotor, modifications of both the Euler work and losses due to skew, i.e. their balance, must be considered. This can be carried out by CFD-based modern turbomachinery design systems.

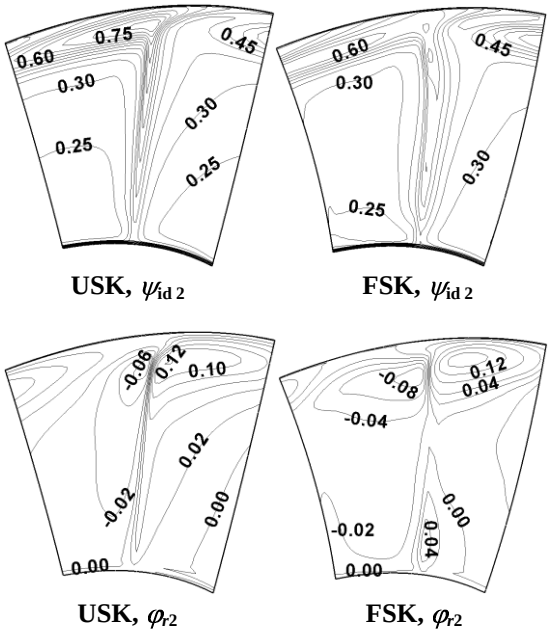

Figure 15. Outlet flow characteristics

5.2. Forward Sweep/Skew vs. Stall

The conclusions of the present paper fit to the former experiences reported in [7] that forward sweep/skew moderates the radial outward migration of the SS boundary layer fluid, and thus, it prevents the near-tip zone from accumulation of stagnating fluid that would lead to tip stalling. Although it was not mentioned in [3][6][7], the applied CVD concept usually intensifies the radial outward flow on the SS, due to shed vorticity. Therefore, the risk of tip stalling is increased for rotors of CVD, and thus, application of forward sweep/skew is especially welcome.

Based on the discussion in [19], it can be concluded that application of forward sweep/skew is especially recommended for CVD rotors to moderate the near-tip stagnating zone.

5.3. Forward Sweep/Skew vs. CVD

As the results presented in the paper indicated, forward sweep/skew reduces the blade load near the tip, and shifts the blade load away from the endwall. This trend is characteristic for near-endwall blade sections with positive sweep [5]. As far as the CVD concept is concerned, this effect acts against it. The results show that the original non-free vortex circulation distribution tends towards that of a free vortex flow pattern (zero spanwise circulation gradient) along the dominant part of span. Therefore, the designer intending to improve the utilisation of blade sections at higher radii (and/or to moderate the load near the blade root for hub loss reduction) by means of CVD must consider the above effect. If no sweep/skew correction is applied to the blade in order to retain the original Euler work distribution, the final result can be a nearly free vortex rotor with reduced efficiency due to off-design incidence.

6. SUMMARY

Comparative CFD studies have been carried out on two rotors in order to investigate the combined effects of CVD and FSK, with use of structured hexahedral meshing. The results are summarised as follows.

1. It has been found that the skewed blade tip protrudes into the upstream relative flow field, and carries out work in advance compared to the blade sections at lower radii. This results in increased and decreased inlet axial velocities near the tip and away from the tip, respectively. The decreased axial velocity at lower radii leads to increased incidence, lift, blade performance, and losses. Forward skew performs an "inward-guiding" effect on the flow in the entire passage. The case study presented herein calls the attention that forward blade skew may cause increased losses along the dominant part of span.

2. It has been pointed out that forward blade skew near the tip moderates the radial outward flow and the losses; although it must be acknowledged that the Euler work near the tip has also been reduced. It was concluded that forward sweep/skew is especially beneficial for CVD rotors in order to reduce the otherwise intensified SS radial outward flow, and thus, to moderate the near-tip stagnating zone.

3. The results showed that forward skew near the tip unloads the near-tip region and uploads the blade at lower radii. This behaviour acts against the CVD concept by reducing the spanwise blade circulation gradient. This fact must be considered in CVD, possibly by correcting the blade in order to retain the original Euler work distribution.

ACKNOWLEDGEMENTS

This work has been supported by the Hungarian National Fund for Science and Research under contracts No. OTKA T 037651and K63704, and, on the behalf of J. Vad, out of the István Széchenyi Fellowship under contract No. SZÖ 271/2003.

REFERENCES

[1] Gallimore, S. J., Bolger, J. J., Cumpsty, N. A., Taylor, M. J., Wright, P. I. and Place, J. M. M., 2002, „The Use of Sweep and Dihedral in Multistage Axial Flow Compressor Blading" – Parts I and II, *ASME J Turbomachinery*, Vol. 124, pp. 521-541.

[2] Corsini, A. and Rispoli, F., 2004, "Using Sweep to Extend the Stall-Free Operational Range in Axial Fan Rotors", *Proc. Instn Mech. Engrs, Part A, J Power and Energy*, Vol. 218, pp. 129-139.

[3] Meixner, H. U., 1995, „Vergleichende LDA-Messungen an ungesichelten und gesichelten Axialventilatoren", *Dissertation Universität Karlsruhe*, VDI-Verlag, Reihe 7, No. 266, Düsseldorf.

[4] Lakshminarayana, B., 1996, *Fluid Dynamics and Heat Transfer of Turbomachinery*, John Wiley & Sons, Inc.

[5] Clemen, C. and Stark, U., 2003, "Compressor Blades with Sweep and Dihedral: a Parameter Study", Proc. *5th European Conference on Turbomachinery Fluid Dynamics and Thermodynamics*, Prague, pp. 129-139.

[6] Beiler, M. G., and Carolus, T.H., 1999, "Computation and Measurement of the Flow in Axial Flow Fans with Skewed Blades", *ASME J Turbomachinery*, Vol. 121, pp. 59-66.

[7] Yamaguchi, N., Tominaga, T., Hattori, S., and Mitsuhashi, T., 1991, "Secondary-Loss Reduction by Forward-Skewing of Axial Compressor Rotor Blading", Proc. *Yokohama International Gas Turbine Congress*, Yokohama, pp. II.61-II.68.

[8] Vad, J., Kwedikha, A. R. A., Kristóf, G., Lohász, M. M., Rábai, G., Rácz, N., 2005, „Effects of Blade Skew in an Axial Flow Rotor of Controlled Vortex Design", Proc. *6th European Conference on Turbomachinery Fluid Dynamics and Thermodynamics*, Lille, pp. 46-55.

[9] Clemen, C., Gümmer, V., Goller, M., Rohkamm, H., Stark, U. and Saathoff, H., 2004, "Tip-Aerodynamics of Forward-Swept Rotor Blades in a Highly-Loaded Single-Stage Axial-Flow Low-Speed Compressor", *Proc. ISROMAC10*, Honolulu, Paper No. 027.

[10] FLUENT 6.2.16 User's Guide, 2004, Fluent Inc., Lebanon, NH, USA.

[11] Benini, E. and Biollo, R., 2006, „On the Aerodynamics of Swept and Leaned Transonic Compressor Rotors", ASME Paper *GT2006-90547*.

[12] Launder, B. E. and Spalding, D. B., 1972, *Lectures in Mathematical Models of Turbulence*, Academic Press, London

[13] Kader, B., 1993, "Temperature and Concentration Profiles in Fully Turbulent Boundary Layers", *Int J Heat Mass Transfer*, Vol. 24, pp. 1541-1544.

[14] Wu, Y., Chu, W., Lu, X. andZhu, J., 2006, "Behavior of Tip Leakage Flow in an Axial Compressor Rotor", *ASME Paper GT2006-90399*.

[15] F.T.Johnson, E.N.Tinoco and N.J.Yu., 2003, „Thirty Years of Development and Application of CFD at Boeing Commercial Airplanes, Seattle", *AIAA paper* 2003-3439.

[16] Benzley, S.E., Borden, M. and Mitchell, S.A., 2001, "A Refinement Technique for All-Hexahedral Adaptive Meshing," *Proc. 1st MIT Conference on Computational Fluid and Solid Mechanics*, Elsevier Science, pp. 1519-1523

[17] Vad, J., and Bencze, F., 1998, "Three-Dimensional Flow in Axial Flow Fans of Non-Free Vortex Design", *Int J Heat Fluid Flow*, Vol. 19, pp. 601-607.

[18] Vad, J., Kwedikha, A. R. A., and Jaberg, H., 2004, "Influence of Blade Sweep on the Energetic Behavior of Axial Flow Turbomachinery Rotors at Design Flow Rate", *ASME Paper GT2004-53544*.

[19] Vad, J., 2006, "Analytical Modeling of Radial Fluid Migration in the Boundary Layer of Axial Flow Turbomachinery Blades", *ASME Paper GT2006-90523*.